

Figure 2. Diagram of the porphyrinato core in $[\text{Fe}(\text{BH}(\text{Bipy})_2\text{P})(\text{CN})_2]^-$. The perpendicular displacements of each atom (in units of 0.01 Å) from the mean plane of the 24-atom core are displayed. The drawing also illustrates the distortion of the axial ligands from an ideal linear arrangement.

dissolved in fluorobenzene ($\lambda_{\text{max}} = 452, 540 \text{ sh}, 670 \text{ nm}$). Dark blue crystals of $[\text{Fe}(\text{BH}(\text{Bipy})_2\text{P})(\text{CN})_2][\text{K}(\text{C}222)](\text{H}_2\text{O})_3 \cdot \frac{1}{2}\text{C}_6\text{H}_5\text{F}$ (**1**)¹⁹ were obtained by slow diffusion of pentane into fluorobenzene solutions of the dicyano-iron(III) derivative.

An ORTEP representation of the porphyrinate anion $[\text{Fe}(\text{BH}(\text{Bipy})_2\text{P})(\text{CN})_2]^-$ as it exists in the crystals of **1** is displayed in Figure 1. This figure also gives the labeling scheme used for most atoms.

The four $\text{Fe}-\text{N}_p$ (N_p = porphyrinato nitrogen) bond distances range from 1.937 (4) to 1.969 (4) Å. Their mean value of 1.949 (14) Å appears to be shorter than the average values observed in the anionic complex $[\text{Fe}(\text{TPP})(\text{CN})_2]^-$ (2.000 (6) Å) and the neutral complex $[\text{Fe}(\text{TTP})(\text{CN})(\text{py})]$ (1.970 (14) Å). The reason for these short $\text{Fe}-\text{N}_p$ bond distances observed in **1** is not clear yet²⁰ but is probably related to the very significant unsymmetrical ruffling of the porphyrin ring (Figure 2). This ruffling is probably mainly due to the presence of the two cyanide axial ligands and their steric interactions with the bipyridine handles. Due to these interactions the two handles are pushed toward the edge of the porphyrin ring (Figure 1).

Although the pyrrole rings are individually planar, the dihedral angles between their adjacent mean planes range from 24.0 (4) to 41.1 (3)°. The two nonequivalent Fe-C and C-N bond distances are not significantly different; the mean values of these bond lengths are respectively 1.949 (4) and 1.152 (9) Å. However, both Fe-CN groups are slightly bent; the corresponding bend angles are respectively $\theta(\text{Fe}-\text{C}85-\text{N}86) = 170.2$ (5)° and $\theta(\text{Fe}-\text{C}87-\text{N}88) = 171.3$ (5)°. Moreover, both Fe-C bonds are tilted off the normal to the 24-atom-core mean plane of the ring; the corresponding tilt angles are respectively $\varphi(\text{Fe}-\text{C}85) = 5.3$ ° and $\varphi(\text{Fe}-\text{C}87) = 5.1$ °. The tilt angles with respect to the normal to the 4 N_p mean plane are respectively 5.9 (Fe-C85) and 4.0° (Fe-C87). The deviations of the two C-N vectors with respect

to the planes defined by the normal to the 24-atom-core mean plane and the two Fe-C vectors are very small.

Due to these distortions from ideal geometry, the cyano carbon atoms C85 and C87 are displaced respectively by 0.18 and 0.17 Å away from the normal to the 24-atom-core mean plane while the cyano nitrogen atoms are displaced respectively by 0.48 and 0.45 Å from this normal. The observed distortions of the Fe-CN groups in **1** are similar to those observed in the crystal structure of $[\text{Mn}^{\text{III}}(\text{TPP})(\text{CN})\text{CHCl}_3]$.³ However, whereas in the manganese(III) complex they result only from intermolecular packing interactions, in **1** they are due mainly to intramolecular steric interactions of the cyano nitrogens N86 and N88 with the bipyridine handles. The closest contacts are $\text{N}86 \cdots \text{C}40$ (3.00 Å), $\text{N}86 \cdots \text{N}41$ (3.04 Å), $\text{N}88 \cdots \text{C}68$ (3.18 Å), and $\text{N}88 \cdots \text{N}75$ (3.22 Å). However, for N88 a strong hydrogen bond with the water molecule OW_1 occurs also; the corresponding $\text{N}88 \cdots \text{OW}_1$ distance is 2.82 Å.

The two bipyridine handles are in a nonplanar trans conformation. The dihedral angles between the mean planes of the pyridine moieties are respectively 39.2 (2) and 43.7 (2)° in the two bipyridine groups. Due to the steric constraints introduced by the two cyano groups, the handles are pushed toward the edge of the porphyrin ring and the mean planes of the bipyridine groups are almost perpendicular to the 24-atom-core mean plane (Figure 1). The very pronounced unsymmetrical ruffling of the porphyrinato core is probably related to these unsymmetrical orientations of the two handles relative to the normal of the 24-atom-core mean plane of the porphyrin.²¹

Acknowledgment. We thank Dr. A. De Cian for his assistance in the X-ray data collection.

Supplementary Material Available: Non-hydrogen atom coordinates (Table S1), anisotropic thermal parameters (Table S2), hydrogen atom coordinates (Table S3), and a complete set of bond lengths (Table S4) and bond angles (Table S5) (19 pages); observed and calculated structure factor amplitudes for all observed reflections (Table S6) (22 pages). Ordering information is given on any current masthead page.

- (21) In $[\text{Zn}(\text{BH}(\text{Bipy})_2\text{P})]$, the two bipyridine handles present a quasi-planar trans conformation and lie almost parallel to the 24-atom-core mean plane of the porphyrin ring. The ruffling of the porphyrin is much less important than in the iron derivative. The dihedral angles between the adjacent mean planes of the pyrrole rings range from 9.1 to 11.8° (average ≈ 10.6 °). The $\text{Zn}-\text{N}_p$ distances have the normal expected values (average $\text{Zn}-\text{N}_p$ 2.030 (14) Å). Schappacher, M.; Fischer, J.; Doppelt, P.; Weiss, R. To be submitted for publication.
- (22) Laboratoire de Cristallographie et de Chimie Structurale (UA 424, CNRS).

Institut Le Bel²²
 Université Louis Pasteur
 4, rue Blaise Pascal
 67070 Strasbourg Cedex, France

Michèle Schappacher
 Jean Fischer
 Raymond Weiss*

Received May 27, 1988

Identification of a Soluble Form of Colloidal Manganese(IV)

For several decades it has been known that many permanganate reactions carried out in both aqueous¹ and organic media² lead to the formation of a soluble brown-yellow manganese species whose UV-vis spectrum shows a broad band with absorbance uniformly decreasing as wavelength increases. Despite its extensive occurrence, identification of this species has not been so far possible, and a survey of the permanganate literature reveals that what appears to be the same species (from both aspect and the

(19) $[\text{Fe}(\text{CN})_2\text{BH}(\text{Bipy})_2\text{P}][\text{K}(\text{C}222)](\text{H}_2\text{O})_3 \cdot \frac{1}{2}\text{C}_6\text{H}_5\text{F}$: $M_r = 1714.7$, space group $P2_1/c$, $a = 14.089$ (2) Å, $b = 24.161$ (4) Å, $c = 25.525$ (4) Å, $\beta = 105.05$ (2)°, $V = 8390.7$ Å³, $Z = 4$, $D_c = 1.35 \text{ g cm}^{-3}$. Data were collected on a Philips PW1100/16 automatic diffractometer in the range $4^\circ < \theta < 57^\circ$ at -100 °C using a single crystal of dimensions $0.20 \times 0.28 \times 0.32 \text{ mm}^3$. The 9120 measured reflections yielded 5502 observations with $I > 3\sigma(I)$. The full-matrix refinement conducted using these reflections and the coordinates obtained from Patterson and Fourier syntheses yielded agreement factors for $R_1 = 0.049$ and $R_2 = 0.071$ (GOF = 1.43). Hydrogen atoms were introduced in structure factor calculations by their computed coordinates (C-H = 0.95 Å) and isotropic temperature factors such as $B(\text{H}) = 1.3[B(\text{X})]$ but not refined. Fluorobenzene and water hydrogens were omitted.

(20) The electronic structure of this ferric porphyrin is presently under study by EPR and Mössbauer spectroscopy.

(1) Freeman, F. *Rev. React. Species Chem. React.* **1976**, *1*, 179.

(2) Lee, D. G. In *Oxidation in Organic Chemistry*; Trahanovsky, W. S., Ed.; Academic Press: New York, 1982; Part D, p 175.

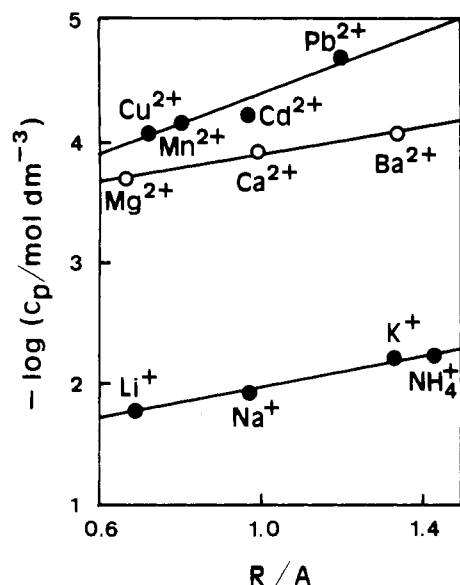


Figure 1. Logarithm of the concentration of cation necessary for precipitating manganese dioxide from a Mn(IV) solution (2.0×10^{-4} mol dm^{-3}) against the cationic radius. All of the electrolytes were in the chloride form.

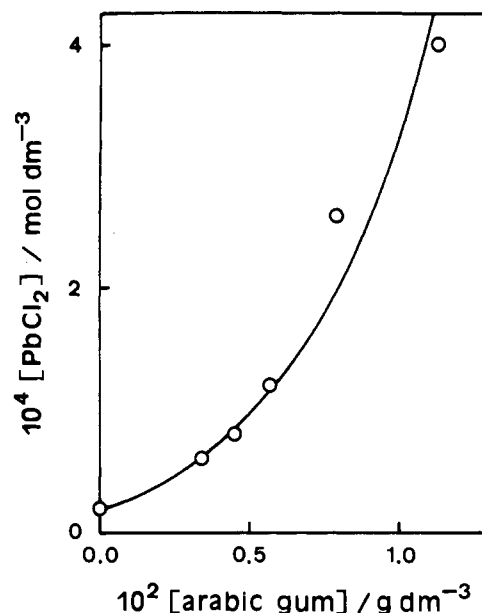
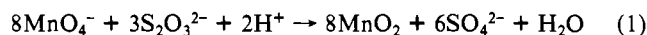


Figure 2. Concentration of lead(II) chloride necessary for precipitating manganese dioxide from a Mn(IV) solution (2.0×10^{-4} mol dm^{-3}) against the arabic gum concentration.

UV-vis spectrum) has received a number of different denominations depending on the nature of the chemical used to reduce permanganate and the existence or not of buffers in the medium. Among others, Mn(III)³ and Mn(V)⁴ reaction intermediates, as well as several Mn(IV) species such as H₂MnO₃,⁵ H₂MnO₄²⁻,⁶ and an undefined Mn(IV)-phosphate complex,⁷ have been proposed as possible chemical formulas for the substance detected. More recently it has been suggested that this species might be a soluble form of colloidal manganese dioxide,⁸ but due to the lack of a clear-cut demonstration some doubts about this interpretation have arisen.⁹

We now report direct evidence for this species being a soluble form of colloidal manganese(IV). Potassium permanganate was reduced by sodium thiosulfate in neutral aqueous solution according to the following stoichiometry:



The experimental reductant/oxidant ratio was 0.39 ± 0.01 . In the experiments performed to determine the stoichiometry the concentration of permanganate was 4.0×10^{-4} mol dm^{-3} and that of thiosulfate ranged from 2.5×10^{-5} to 4.0×10^{-4} mol dm^{-3} . The soluble Mn(IV) species obtained was dark brown, and the solutions remained perfectly transparent, precipitation not having been observed even after several months had elapsed. Thus phosphate buffers were not needed to keep the Mn(IV) species in solution.⁷ The UV-vis spectrum indicated that this species was the same that had been previously detected in many permanganate reactions.³⁻⁹

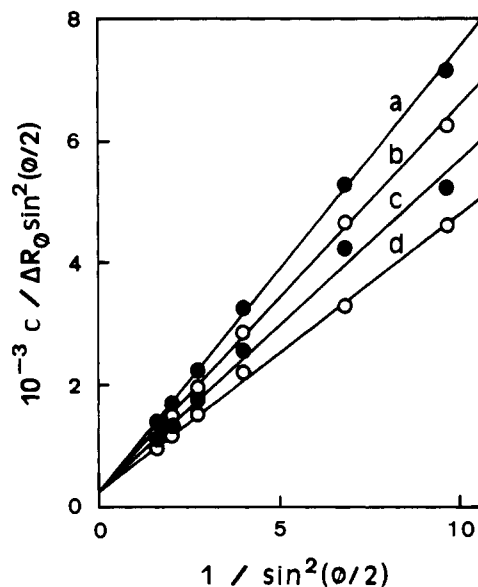


Figure 3. Results from nephelometry. ΔR_ϕ is the Rayleigh scattering increment observed at a wavelength of 546 nm for several colloid concentrations, c , and different scattering angles, ϕ . $[\text{MnO}_2] = 8.30$ (a), 5.53 (b), 2.77 (c), and 0 (d, extrapolated) $\times 10^{-3}$ g dm^{-3} .

Precipitation of manganese dioxide was observed when the initially transparent solutions were stirred in the presence of different electrolytes. In Figure 1 the negative logarithm of the minimum concentration of several chlorides necessary for precipitation of manganese dioxide has been plotted against the cationic radius. We can see that the resulting points can be fitted along three different straight lines depending on their corresponding to monovalent ions, divalent ions from alkaline-earth metals, or divalent ions from other metals. Divalent ions are better coagulating agents than monovalent ones; moreover, for cations with identical charge, the coagulating efficiency increases with the ionic radius.

While a change of cation implies a different efficiency of the corresponding electrolyte as coagulating agent, the same does not apply as far as the anion is concerned. For example, equivalent amounts of sodium ion are necessary whether the electrolyte used is NaCl (1.2×10^{-2} mol dm^{-3}), NaNO₃ (1.2×10^{-2} mol dm^{-3}), or Na₂SO₄ (6.0×10^{-3} mol dm^{-3}). On the other hand, addition of a protective colloid results in an increase in the concentration

- (3) Senet, S.; Martin, M. *An. Quim.* **1960**, 56B, 123.
- (4) (a) Lee, D. G.; Brownridge, J. R. *J. Am. Chem. Soc.* **1973**, 95, 3033. (b) Wiberg, K. B.; Deütsch, C. J.; Rocek, J. *Ibid.* **1973**, 95, 3034. (c) Lee, D. G.; Brownridge, J. R. *Ibid.* **1974**, 96, 5517. (d) Lee, D. G.; Brown, K. C. *Ibid.* **1982**, 104, 5076. (e) Freeman, F.; Fuselier, C. O.; Karchefski, E. M. *Tetrahedron Lett.* **1975**, 2133.
- (5) (a) Simandi, L. I.; Jaky, M. *J. Am. Chem. Soc.* **1976**, 98, 1995. (b) Freeman, F.; Fuselier, C. O.; Armstead, C. R.; Dalton, C. E.; Davidson, P. A.; Karchefski, E. M.; Krochman, D. E.; Johnson, M. N.; Jones, N. K. *Ibid.* **1981**, 103, 1154. (c) Simandi, L. I.; Jaky, M.; Freeman, F.; Fuselier, C. O.; Karchefski, E. M. *Inorg. Chim. Acta* **1978**, 31, L457.
- (6) Stewart, R. In *Oxidation in Organic Chemistry*; Wiberg, K. B., Ed.; Academic Press: New York, 1965; Part A, p 6.
- (7) Wiberg, K. B.; Stewart, R. *J. Am. Chem. Soc.* **1955**, 77, 1786.
- (8) (a) Freeman, F.; Kappos, J. C. *J. Am. Chem. Soc.* **1985**, 107, 6628. (b) Mata, F.; Perez-Benito, J. F. *Can. J. Chem.* **1985**, 63, 988. (c) Perez-Benito, J. F.; Lee, D. G. *Ibid.* **1985**, 63, 3545.
- (9) Simandi, L. I.; Jaky, M.; Savage, C. R.; Schelly, Z. A. *J. Am. Chem. Soc.* **1985**, 107, 4220.

of electrolyte necessary for precipitation to occur, as exemplified in Figure 2 for arabic gum as protective colloid and PbCl_2 as coagulating agent.

All these results suggest that the soluble Mn(IV) species is present in the medium in the form of colloidal particles of manganese dioxide with a negative electrostatic charge, which accounts for their stability in solution, due to the adsorption of anions (such as sulfate ions, for instance) on their surface. When an electrolyte is added, adsorption of the cation on the colloidal particles results in neutralization of their electrostatic charge; i.e., precipitation occurs. Divalent ions are more attracted by the negatively charged particles than monovalent ones, while for the same ionic charge adsorption will be easier for the less solvated bigger cations. Furthermore, when the colloidal particles are protected by arabic gum, the adsorption of cations on their surface is considerably more difficult.

Finally, the colloidal particles of this soluble form of manganese(IV) have been characterized by the use of a conventional nephelometric technique whose results are shown in Figure 3. From this study it follows that the colloidal particles are roughly spherical with a radius around 500 Å and a mass of 2×10^8 g mol⁻¹.

To the best of our knowledge this is the first time that the existence of a soluble form of colloidal manganese(IV) has been unquestionably proved. This might bear important consequences in relation to mechanistic and kinetic studies involving this species as a reactant¹⁰ or as an autocatalytic product.¹¹

Registry No. Mn, 7439-96-5; KMnO_4 , 7722-64-7; $\text{Na}_2\text{S}_2\text{O}_3$, 7772-98-7.

- (10) Jaky, M.; Simandi, L. I.; Shafirovich, V. Y. *Inorg. Chim. Acta* **1984**, *90*, L39.
 (11) (a) Lee, D. G.; Perez-Benito, J. F. *Can. J. Chem.* **1985**, *63*, 1275. (b) Perez-Benito, J. F.; Mata, F.; Brillas, E. *Ibid.* **1987**, *65*, 2329. (c) Mata, F.; Perez-Benito, J. F. *Ibid.* **1987**, *65*, 2373. (d) Mata, F.; Perez-Benito, J. F. *J. Chem. Educ.* **1987**, *64*, 925. (e) de Andres, J.; Brillas, E.; Garrido, J. A.; Perez-Benito, J. F. *J. Chem. Soc., Perkin Trans. 2* **1988**, 107. (f) Perez-Benito, J. F. *J. Chem. Soc., Chem. Commun.* **1987**, 831.

Departamento de Quimica Fisica
 Facultad de Quimica
 Universidad de Barcelona
 Marti i Franques, 1
 08028-Barcelona, Spain

Joaquin F. Perez-Benito*
 Enrique Brillas

Departamento de Fisico-Quimica
 Aplicada
 Facultad de Farmacia
 Universidad de Barcelona
 Avenida Diagonal, 643
 08028-Barcelona, Spain

Ramon Poupiana

Received July 15, 1988

Solid-State Chalcogenide Anions of Ta and Nb: Synthesis and Structures of the $\text{Ta}_2\text{S}_{11}^{4-}$ and $\text{Nb}_4\text{Se}_{22}^{6-}$ Anions

An extensive set of soluble polynuclear metal sulfides of Mo^{1-6} and W^{7-11} has been obtained, most derived from the simple

- (1) MoS_9^{2-} : (a) Simhon, E. D.; Baenziger, N. C.; Kanatzidis, M.; Draganjac, M.; Coucouvanis, D. *J. Am. Chem. Soc.* **1981**, *103*, 1218-1219. (b) Draganjac, M.; Simhon, E.; Chan, L. T.; Kanatzidis, M.; Baenziger, N. C.; Coucouvanis, D. *Inorg. Chem.* **1982**, *21*, 3321-3332.
 (2) $\text{Mo}_2\text{S}_8^{2-}$: Pan, W.-H.; Harmer, M. A.; Halbert, T. R.; Stiefel, E. I. *J. Am. Chem. Soc.* **1984**, *106*, 459-460.
 (3) $\text{Mo}_2\text{S}_{10}^{2-}$: Clegg, W.; Christou, G.; Garner, C. D.; Sheldrick, G. M. *Inorg. Chem.* **1981**, *20*, 1562-1566.
 (4) $\text{Mo}_2\text{S}_{12}^{2-}$: (a) Müller, A.; Bhattacharyya, R. G.; Pfefferkorn, B. *Chem. Ber.* **1979**, *112*, 778-780. (b) Müller, A.; Nolte, W. O.; Krebs, B. *Inorg. Chem.* **1980**, *19*, 2835-2836.
 (5) $\text{Mo}_3\text{S}_9^{2-}$: Pan, W.-H.; Leonowicz, M. E.; Stiefel, E. I. *Inorg. Chem.* **1983**, *22*, 672-678.

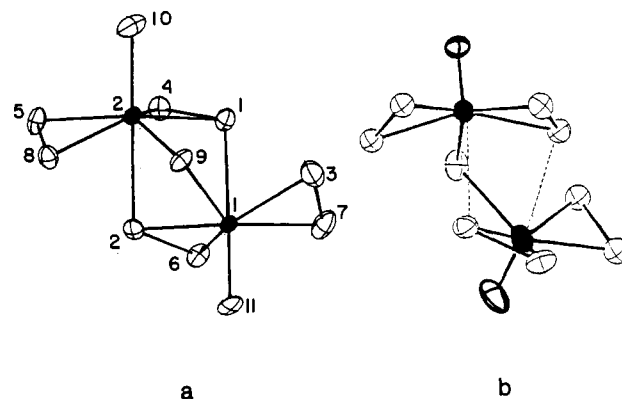


Figure 1. Structure of the $\text{Ta}_2\text{S}_{11}^{4-}$ ion (a) in comparison to that of the $\text{Mo}_2\text{S}_9\text{O}_2^{2-}$ ion (b).²⁵ In this figure and in Figure 2 85% probability ellipsoids are shown in part a, while 40% ellipsoids are shown in part b. The metal is represented as a black ellipsoid, and oxygen is represented as a darkened ellipsoid, while all remaining ellipsoids are sulfur or selenium.

MS_4^{2-12} unit ($M = \text{Mo}, \text{W}$). The corresponding mononuclear selenides $\text{MSe}_4^{2-13,14}$ are known, and there is a growing list of other mononuclear¹⁵ and polynuclear¹⁶ selenides. In contrast, the only known soluble discrete sulfur anions of Nb and Ta are $\text{M}'_6\text{S}_{17}^{4-}$ ($M' = \text{Nb}, \text{Ta}$)¹⁷ and there are no examples of soluble selenium species. Although the VS_4^{3-} anion¹⁸ exists in solution, it has not yet been shown to be a precursor to polynuclear species that contain only V and S. But for $M' = \text{Nb}$ and Ta, discrete $\text{M}'\text{Q}_4^{3-}$ anions ($Q = \text{S}, \text{Se}$) have not been obtained in solution. Solid-state chemistry provides a valuable but often forgotten route to coordination compounds, especially where the transition metal is in a high oxidation state. One example is the production of Na_2CrO_4 by fusion of chromite (FeCr_2O_4) with Na_2CO_3 in air. Indeed, the existence of the NbQ_4^{3-} and TaQ_4^{3-} anions has been established in the solid state ($\text{Cu}_3\text{M}'\text{S}_4$,¹⁹ $\text{Tl}_3\text{M}'\text{S}_4$,²⁰ $\text{Ba}_6[\text{NbS}_4][\text{NbS}_3\text{O}]_3$,²¹ and $\text{Cs}_3\text{M}'\text{Se}_4$).²² By solid-state means we have prepared in

- (6) $\text{Mo}_3\text{S}_{13}^{2-}$: Müller, A.; Pohl, S.; Dartmann, M.; Cohen, J. P.; Bennett, J. M.; Kirchner, R. M. *Z. Naturforsch., B: Anorg. Chem., Org. Chem.* **1979**, *34B*, 434-436.
 (7) $\text{W}_3\text{S}_8^{2-}$: (a) Müller, A.; Bögge, H.; Krickemeyer, E.; Henkel, G.; Krebs, B. *Z. Naturforsch., B: Anorg. Chem., Org. Chem.* **1982**, *37B*, 1014-1019. (b) Müller, A.; Rittner, W.; Neumann, A.; Königler-Ahlborn, E.; Bhattacharyya, R. G. *Z. Anorg. Allg. Chem.* **1980**, *461*, 91-95. (c) Sécheresse, F.; Lavigne, G.; Jeannin, Y.; Lefebvre, J. *J. Coord. Chem.* **1981**, *11*, 11-16.
 (8) $\text{W}_2\text{S}_{11}^{2-}$: Manoli, J. M.; Potvin, C.; Sécheresse, F. *Inorg. Chem.* **1987**, *26*, 340-341.
 (9) $\text{W}_2\text{S}_{11}\text{H}^-$: Sécheresse, F.; Manoli, J. M.; Potvin, C. *Inorg. Chem.* **1986**, *25*, 3967-3971.
 (10) $\text{W}_3\text{S}_8^{2-}$: Bhaduri, S.; Ibers, J. A. *Inorg. Chem.* **1986**, *25*, 3-4.
 (11) $\text{W}_4\text{S}_{12}^{2-}$: Sécheresse, F.; Lefebvre, J.; Daran, J. C.; Jeannin, Y. *Inorg. Chem.* **1982**, *21*, 1311-1314.
 (12) Müller, A.; Diemann, G.; Jostes, R.; Bögge, H. *Angew. Chem., Int. Ed. Engl.* **1981**, *20*, 934-955 and references therein.
 (13) Müller, A.; Krebs, B.; Diemann, E. *Angew. Chem., Int. Ed. Engl.* **1967**, *6*, 257-258.
 (14) Lenher, V.; Fruekas, A. G. *J. Am. Chem. Soc.* **1927**, *49*, 3076-3080.
 (15) $\text{MQ}(\text{Se}_4)_2^{2-}$: Wardle, R. W. M.; Mahler, C. H.; Chau, C.-N.; Ibers, J. A. *Inorg. Chem.* **1988**, *27*, 2790-2795; O'Neal, S. C.; Kolis, J. W. *J. Am. Chem. Soc.* **1988**, *110*, 1971-1973.
 (16) $\text{W}_3\text{Se}_8^{2-}$, $\text{W}_2\text{Se}_7^{2-}$, $\text{W}_2\text{Se}_{10}^{2-}$: Wardle, R. W. M.; Chau, C.-N.; Ibers, J. A. *J. Am. Chem. Soc.* **1987**, *109*, 1859-1860. Wardle, R. W. M.; Bhaduri, S.; Chau, C.-N.; Ibers, J. A. *Inorg. Chem.* **1988**, *27*, 1747-1755.
 (17) Sola, J.; Do, Y.; Berg, J. M.; Holm, R. H. *Inorg. Chem.* **1985**, *24*, 1706-1713.
 (18) Muller, M.; Leroy, M. J. F.; Rohmer, R. C. R. *Seances Acad. Sci., Ser. C* **1970**, *270*, 1458-1460.
 (19) Hulliger, F. *Helv. Phys. Acta* **1961**, *34*, 379-382.
 (20) Crevecoeur, C. *Acta Crystallogr.* **1964**, *17*, 757.
 (21) Rendon-Diazmiron, L. E.; Campana, C. F.; Steinfink, H. *J. Solid State Chem.* **1983**, *47*, 322-327.
 (22) Yun, H.; Randall, C. R.; Ibers, J. A. *J. Solid State Chem.* **1988**, *76*, 109-114.